Improving binding potential analysis in [^{11}C]raclopride PET studies using cluster analysis

Gerhard Glatting[a] and Felix M. Mottaghy
Department of Nuclear Medicine, University of Ulm, 89070 Ulm, Germany

Jochen Karitzky
Department of Neurology, University of Ulm, 89070 Ulm, Germany

Axel Baune
Department of Neuroinformatics, University of Ulm, 89070 Ulm, Germany

Friedrich T. Sommer
Redwood Neuroscience Institute, Menlo Park, California 94025

G. Bernhard Landwehrmeyer
Department of Neurology, University of Ulm, 89070 Ulm, Germany

Sven N. Reske
Department of Nuclear Medicine, University of Ulm, 89070 Ulm, Germany

(Received 18 July 2003; revised 16 January 2004; accepted for publication 20 January 2004; published 23 March 2004)

To calculate binding potentials (BP) in [^{11}C]raclopride brain PET studies a reference tissue model is widely used. The aim of the present study was to improve the determination of time activity curves (TAC) of reference tissue regions using cluster analysis. In four patients with Huntington disease TACs of a cerebellar reference region were calculated either from manually placed circular ROIs within the cerebellum or by cluster analysis. BP estimates derived from cluster analysis are independent from inter- and intraobserver variations and show an improved reproducibility combined with a low variability compared to manually placed cerebellar ROIs. This is of high value in longitudinal studies. © *2004 American Association of Physicists in Medicine.*
[DOI: 10.1118/1.1668392]

Key words: PET, binding potential, cluster analysis, raclopride, reference region

I. INTRODUCTION

[^{11}C]raclopride and positron emission tomography (PET) are used to determine dopamine D_2-receptor binding sites in vivo.[1–3] For quantitative analysis of clinical [^{11}C]raclopride PET studies a reference tissue model has been shown to be valid and is widely used in order to avoid arterial blood sampling.[4] This model requires one to collect time activity curves (TACs) of a reference region, conventionally the cerebellum. The reference tissue model assumes that the region selected as reference tissue does not contain specific binding sites, i.e., dopamine D_2-receptor-like binding sites. There is evidence, however, that lobules 9 and 10 of the vermis of the cerebellum express dopamine D_3-receptors known to bind raclopride,[5] at least in rats.[6–8] In addition, an immunohistochemical study suggested the presence of D_2-like immunoreactivity in the cerebellum.[9]

The standard method to determine a TAC for a reference tissue involves the manual definition of a region of interest (ROI) as reference region. It is obvious that, aside from inadvertedly included regions containing specific binding, focal inhomogeneities in blood flow and blood brain barrier permeability increase variability in manually defined reference tissue ROIs. Cluster analysis is set to automatically identify volume elements (voxels) with similar biokinetics of a given tracer.[10–13]

The aim of the present study was to assess whether it is feasible to employ cluster analysis to identify homogeneous tissue reference regions in PET studies using [^{11}C]raclopride. Manually defined ROIs were applied as a reference.

II. METHODS

Four patients with the genetically confirmed diagnosis of Huntington disease (HD) in early clinical stages of the disease, who participated in a longitudinal [^{11}C]raclopride study, were enrolled (one female, three males; mean age 50 years, range 40–56) and investigated twice (delay 15.8 months, range 15.6–16.1). The study was approved by the local ethical review board. All patients signed informed consent forms prior to PET examination.

PET data were acquired dynamically in 3D mode (Siemens/CTI ECAT EXACT HR+, Knoxville, TN).[14] Subjects were positioned in the scanner using a vacuum pillow by which an individually formed head mold was generated. The head was aligned parallel to the orbitomeatal line with the aid of an external laser beam. To correct for attenuation a transmission scan of 10 min duration was performed using a retractable ^{68}Ga/^{68}Ge source. [^{11}C]raclopride [doses: (247 ± 27) MBq; specific activity (29 ± 15) GBq/μmol] in 10 ml sterile physiological saline was injected as a bolus. A dy-

namic PET protocol with 17 temporal frames with a duration between 5 and 600 s over 60 min was used starting at the time of injection. Reconstruction was performed using the PROMIS (PROject Missing Sinograms) algorithm of the manufacturer with a cutoff of 0.5. This algorithm first calculates a forward projection from the two-dimensional data for the event positions beyond the physical field-of-view followed by 3D filtered backprojection.[15]

Binding potential (BP) is estimated using a simplified reference region model.[4,16] This model requires a reference region devoid of specific binding and derives the BP from the ratio of volumes of distribution of the ligand in the striatum relative to the cerebellum according to[12,17]

$$\mathrm{BP}=\frac{f_2 B_{\max}}{K_D(1+\Sigma_i F_i/K_{Di})} \tag{1}$$

f_2 is the free fraction of unbound ligand in the tissue, $B_{\max}$ is the total concentration of specific binding sites, and K_{D} and K_{Di} are the equilibrium dissociation constants of the ligand and i competing endogenous ligands. F_i are the corresponding concentrations. The receptor parametric mapping (RPM) software developed by Gunn *et al.*[16] was used to determine the BP. This software implements a basis function method for the simplified reference tissue model at the voxel level[4,16] to enable a fast and robust solution. The introduction of the basis set allows us to use realistic parameter bounds, which makes the model robust at the voxel level. As input the software needs the TAC of the reference region devoid of specific binding.[16]

Two approaches were used to define the TAC of the reference region. First, the cerebellar time activity curve was determined from the mean of six circular regions of interest (ROI), manually placed on three subsequent planes covering the region of the cerebellar hemispheres.[18] Second, cluster analysis was used to partition voxel time activity curves into a small number of clusters.[11] Only voxels with an activity larger than the mean in the image were included in the analysis in order to exclude voxels outside the patient or those with very low activity in the liquor. The different frames j of a study were weighted according to Poisson statistics[16] with the factor

$$w_j=(\text{frame } j \text{ duration})^2/(P_j+D_j). \tag{2}$$

The prompts P_j are the total counts obtained for frame j. The counts measured in the delayed coincidence window D_j are subtracted to obtain the true coincidences T_j $(=P_j-D_j)$. [Note that the variance (V) of the difference of two Poisson variables equals the sum of the variables, i.e., $V(T_j)=P_j+D_j$.] The frame duration is included because the data in the reconstructed images contain ''counts per frame duration.'' The benefit of weighting is that the frames contribute according to their statistical weight. This prevents low count frames from dominating the clustering process.[11] The remaining set of signal time courses was analyzed using the classical k-means cluster analysis algorithm with setting $k=10$.[19] This adaptive hard-clustering algorithm uses the mean quadratic quantization error (MQQE) as validation measure. With hard clustering the membership to cluster centers is a disjunct partition of the data. The MQQE is defined as

$$\mathrm{MQQE}_k=\frac{1}{N}\sum_{c=1}^{k}\sum_{ic}(x_c-x_{ic})^2 \tag{3}$$

with N the total number of clustered voxels, and x_{ic} the voxel TACs belonging to class prototype x_c. The vectors x contain the time activity curve of the corresponding voxels. Fitting is provided by a gradient descent method. The number k of clusters was determined by trial and error. A problem with k-means cluster analysis is that due to the random initialization process repeated runs yield different results and some can have insufficient goodness of fit due to local minima in the objective function of the method (but see Sec. IV). In order to find good clustering solutions and to check the reproducibility of the results we repeated the cluster analysis for each patient ten times. The mean quadratic quantization error (MQQE) between data points and the according class prototypes served as measure for the goodness of fit. As measure for reproducibility we used the mean and standard deviation of the sizes of the clusters for each replication for all patients. Additionally, the reproducibility (mean and standard deviation) of the striatal binding potentials were determined using the receptor parametric mapping (RPM) software.[16] For this purpose, the striatal cluster of the optimal clustering analysis was used together with all replications of the cerebellar TACs, i.e., the cerebellar clusters and the manually drawn cerebellar ROIs.

Results were compared using the Wilcoxon matched pairs signed rank test using GraphPad Prism version 3.02 for Windows (GraphPad Software, San Diego, CA, www.graphpad.com). The nonparametric Wilcoxon test first computes the differences between the two values of the matched pairs, and analyzes thereafter only the list of differences. The Wilcoxon test does not assume that these differences are sampled from a Gaussian distribution.

III. RESULTS

The TACs of the clusters showed four distinct clusters by visual inspection: venous, striatum, white/gray matter continuum, and scatter. Thus with $k=10$ the clustering algorithm had enough clusters to separate the voxels with partial volume effects into extra clusters. Inspecting the differences of the cluster analyses within one patient with respect to the MQQE showed that those yielding a low MQQE showed the venous system of the brain as a separate cluster (Fig. 1). Subsequent investigations were restricted to the subgroup of analyses with low MQQEs. The results of a detailed analysis with respect to cluster sizes are shown in Table I.

The TACs of the cluster containing the largest part of the cerebellum were used to determine the BP for the striatal cluster using the receptor parametric mapping (RPM) software.[16] A comparison with the manually drawn (cerebellar) ROIs method is given in Table II. An example for the TACs is given in Fig. 2.

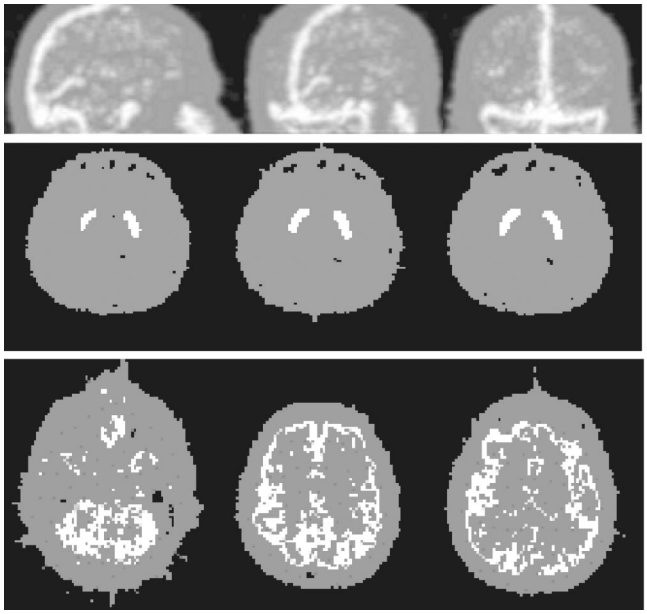

FIG. 1. Examples for ''venous'' cluster (top; maximum intensity projection for three angles), ''striatal'' (middle) and ''cerebellar'' (bottom; axial slices) cluster.

To quantify a suspected presence of D_2-like immunoreactivity[9] in the manually drawn cerebellar ROIs, we calculated the BP of the manually drawn cerebellar ROIs using the cerebellar cluster as reference region. The obtained binding potential was 0.04 ± 0.04 and range was 0.00 to 0.12 (for patient 2 a fit could not be obtained, therefore the BP was assumed to be zero).

IV. DISCUSSION

The reproducible generation of parametric PET images depends on the definition of an appropriate reference tissue TAC devoid of specific binding.[4,12] For [^{11}C]raclopride PET studies, a reference tissue model is widely used and regarded as valid,[4] which requires the delineation of a reference region. Conventionally the cerebellum is used as a reference region with the implicit assumption that this region does not contain specific binding sites. However, as discussed in the Introduction, there is evidence for the presence of D_2-like binding sites in certain regions of the cerebellum. Cluster analysis allows the inclusion of additional cortical regions with the same TACs as the cerebellum. This increased size of the reference region reduces noise and improves the determination of the binding potential. In addition, venous blood vessels may contribute to a variable and unpredictable degree to the regional signal of manually delineated cerebellar ROIs.

Both limitations can be overcome using a method able to distinguish different dynamics of TACs. For this purpose we used cluster analysis and demonstrated that a single cluster analysis does not necessarily result in an optimal identification of relevant structures. However, when performing ten arbitrarily initialized cluster analyses, an optimal subgroup showing a venous cluster yields results of high reproducibility with respect to MQQE. We showed that the high MQQE reproducibility corresponds to a high reproducibility of cluster sizes (Table I) and as a consequence TACs (Fig. 2). The high TAC reproducibility transforms directly into BP reproducibility (Table II). Therefore, the optimal method to use this kind of cluster analysis consists in performing ten cluster analyses and utilize that with the lowest MQQE (which

TABLE II. Binding potentials (BPs) assessed using TACs of the cerebellar cluster and the manually drawn cerebellar ROIs (mean $\pm$ SD).

BP by RPM	*N*	Cerebellar cluster	*N*	Cerebellar ROIs
1a	4	0.969 ± 0.002	5	0.891 ± 0.005
1b	5	1.153 ± 0.001	5	1.041 ± 0.006
2a	4	1.387 ± 0.002	5	1.351 ± 0.015
2b	6	1.685 ± 0.005	5	1.477 ± 0.011
3a	4	1.401 ± 0.001	5	1.201 ± 0.039
3b	6	1.281 ± 0.001	5	1.219 ± 0.017
4a	6	0.607 ± 0.001	5	0.396 ± 0.028
4b	4	0.878 ± 0.001	5	0.827 ± 0.022

Note: Of the ten performed clustering analyses those showing the venous cluster (which corresponds to low MQQEs, number *N*) were used. For the manually drawn cerebellar ROIs the TAC was determined independently $N = 5$ times. The BP was calculated using the receptor parametric mapping (RPM) software developed by Gunn *et al.*[16] The Wilcoxon matched pairs signed rank test demonstrates a significant difference between the manually and cluster defined reference tissue ROIs for both the BP and the standard deviation ($p < 0.05$).

TABLE I. Cluster sizes described by voxel numbers (mean $\pm$ SD; 1 voxel = 16 mm^3).

Study	*N*	Cerebellar	Thalamo-cortical	Striatal	Venous	Manually
1a	4	21102 ± 14	15948 ± 76	825.0 ± 2.3	4046 ± 16	685 ± 4
1b	5	22952 ± 31	17117 ± 42	771.8 ± 0.4	5123 ± 31	610 ± 3
2a	4	21391 ± 45	14243 ± 116	882.0 ± 0.0	11568 ± 5	974 ± 4
2b	6	18820 ± 84	18285 ± 110	852.7 ± 1.0	8873 ± 69	860 ± 8
3a	4	19223 ± 11	16391 ± 47	896.0 ± 0.0	6679 ± 8	757 ± 6
3b	6	20488 ± 3	16123 ± 7	893.7 ± 0.8	4720 ± 2	927 ± 4
4a	6	22118 ± 5	18855 ± 11	4735.2 ± 34.9	2677 ± 37	589 ± 3
4b	4	19264 ± 26	14390 ± 19	906.8 ± 5.9	4962 ± 9	683 ± 3

Note: *N* is the number of clustering analyses showing the venous system of the brain as a separate cluster. Differences in mean voxel numbers between investigation a and b are partially due to different patient positioning. For comparison, the sizes of the manually drawn cerebellar ROIs (sum of six circles drawn in three consecutive planes; five replications) are given in the right column. The ''striatal'' cluster of investigation 4a contains additional cortical areas of the brain: The clustering analysis did not separate the striatal area, due to its low binding potential (Table II). On average, the cluster method yields 28 ± 7 times more voxels for the reference region compared to manually determined reference regions.

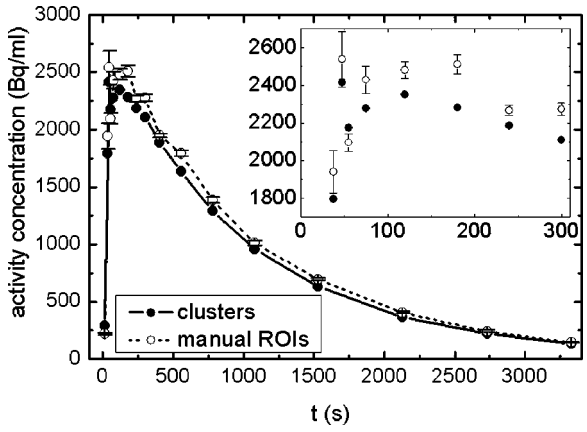

FIG. 2. Comparison of TACs defined by cluster analysis (mean of $N=4$ clustering analyses) and manual ROIs in the cerebellum (mean and SD for $N=5$) for patient 3a. The standard deviation SD for the cluster results is not shown, because it is too small to depict (SD<2 Bq/ml).

shows a venous cluster) in the following evaluation. Thus, variability introduced by the expert through manually defined ROIs is obviated. Note that the variability of the BP for the manually drawn ROIs in Table II is only depicting *intra*observer variability, however in a clinical setting usually *inter*observer variability is more relevant. Therefore, a standardized method defining a reference region is warranted.

Although cluster analysis was already used previously in binding potential analysis[11,12,17] the issue of reproducibility was not demonstrated. We demonstrated the following.

(1) With our clustering algorithm we could obtain in all cases convincing results by multiple runs (in contrast to the statement in Ref. 11).
(2) Due to our Poisson weighting we obviate user interaction to exclude or combine low count frames (compare Ref. 11).
(3) Because we use a hard clustering algorithm instead of the mixture model[11] we do not need/allow user interaction to define the threshold for the probabilities for which the voxels are partitioned into the respective cluster. This avoids additional inter- and intraobserver variability.

The cluster analysis may be improved using a nonrandomized initialization[20,21] or by a dynamical cluster analysis that extracts useful values of k from the data.[13] Our expectation is that with such improvements more than five to six runs (closer to ten) of the analysis runs would yield useful results. However, we did not investigate this point as time is not critical in the BP evaluation. The fraction of useful runs may be increased also by escalating the number of clusters k on the expense of CPU time.

The additional voxels included into the reference region by clustering are distributed over the cortex with a pattern, which is not possible to select manually (compare Fig. 1). Therefore, it is not possible to *simply* enlarge the reference region manually by selecting regions other than those in the cerebellum to obtain the same benefit in reproducibility without clustering. On the other hand, the ''cerebellar'' cluster excludes parts of the cerebellum, which are suspected to contain specific binding sites.[5] The positive BP ($=0.04\pm0.04$) obtained for the manually drawn ROIs using the cerebellar cluster as reference region is compatible with the presence of specific binding sites for raclopride in the region defined by the manually drawn cerebellar ROIs that cannot be neglected. As a consequence the calculated BP was lower when using the manually defined ROI technique (Table II). This supports the assumption that the highly reproducible TACs based on cluster analysis are devoid of major contributions of areas with specific binding. However, this small BP value could also be due to several confounding factors, such as choice of model, e.g., a model using the arterial input function instead of a reference region may yield different results. Or this small BP value could be a systematic artifact of imaging, e.g., of noise in the attenuation maps or of inaccuracies in the scatter correction or normalization. To definitely characterize these small BP values as specific binding a separate D2/D3 saturation study must be performed.

The influence of other image reconstruction algorithms[22–24] like EM-ML (expextation maximization–maximum likelihood), OSEM (ordered subset expectation maximization) and MAP (maximum *a posteriori*)[25] were not investigated. However, provided that the algorithms converged,[25] the relevant differences in the reconstructed images for cluster analysis are the resolution and the noise.[26] A change in resolution affects the degree of the partial volume effect, i.e., a better resolution may need a slightly increased number of clusters to separate the voxels with partial volume effects into extra clusters. The same holds true for increased noise: More clusters allow a reduced ''noise'' within each cluster. If such an adjustment to different reconstruction algorithms would be necessary, it would reduce the number of pixels in the demanded reference cluster. However, the benefit of clustering probably will not be reduced excessively, because the diminished variation within the smaller cluster counteracts the decreased pixel number in the cluster.

The RPM method[16] implements parameter bounds with respect to the simplified reference region model,[4] which in turn reduces the number of free parameters of the reference tissue model from four to three. Although the results are essentially the same[4,16] after this reduction in the degrees of freedom it is clear that a model with more parameters is more sensitive to noise. Therefore, compared to the RPM method the clustering should be even more advantageous for both, the simplified reference region model and the reference tissue model, due to noise reduction in the TAC of the reference region.

In conclusion, the semiautomated and observer independent cluster analysis allows us to analyze *in vivo* receptor binding studies using a reference tissue model with high accuracy and reproducibility.

ACKNOWLEDGMENTS

The authors thank Dr. R. N. Gunn for advice with the implementation of his RPM software. For helpful discussions and support we thank our colleagues Dr. B. Neumaier, Dr. K. Henkel, J. Ruckgaber, and Dr. M. Schmid.

[a]Electronic mail: gerhard.glatting@medizin.uni-ulm.de

[1] A. Antonini, K. L. Leenders, R. Spiegel, D. Meier, P. Vontobel, M. Weigell-Weber, R. Sanchez-Pernaute, J. G. de Yebenez, P. Boesiger, A. Weindl, and R. P. Maguire, ''Striatal glucose metabolism and dopamine D2 receptor binding in asymptomatic gene carriers and patients with Huntington's disease,'' Brain **119**, 2085–2095 (1996).

[2] N. Turjanski, R. Weeks, R. Dolan, A. E. Harding, and D. J. Brooks, ''Striatal D1 and D2 receptor binding in patients with Huntington's disease and other choreas. A PET study,'' Brain **118**, 689–696 (1995).

[3] L. Farde, E. Ehrin, L. Eriksson, T. Greitz, H. Hall, C. G. Hedstrom, J. E. Litton, and G. Sedvall, ''Substituted benzamides as ligands for visualization of dopamine receptor binding in the human brain by positron emission tomography,'' Proc. Natl. Acad. Sci. U.S.A. **82**, 3863–3867 (1985).

[4] A. A. Lammertsma and S. P. Hume, ''Simplified reference tissue model for PET receptor studies,'' Neuroimage **4**, 153–158 (1996).

[5] P. Sokoloff, B. Giros, M. P. Martres, M. L. Bouthenet, and J. C. Schwartz, ''Molecular cloning and characterization of a novel dopamine receptor (D3) as a target for neuroleptics,'' Nature (London) **347**, 146–151 (1990).

[6] J. M. Vessotskie, M. P. Kung, S. Chumpradit, and H. F. Kung, ''Quantitative autoradiographic studies of dopamine D3 receptors in rat cerebellum using [^{125}I]S(−)5-OH-PIPAT,'' Brain Res. **778**, 89–98 (1997).

[7] D. Boulay, R. Depoortere, G. Perrault, and D. J. Sanger, ''Decreased locomotor activity after microinjection of dopamine D2/D3 receptor agonists and antagonists into lobule 9/10 of the cerebellum: a D3 receptor mediated effect?'' Prog. Neuropsychopharmacol. Biol. Psychiatry **24**, 39–49 (2000).

[8] L. Herroelen, J. P. De Backer, N. Wilczak, A. Flamez, G. Vauquelin, and J. De Keyser, ''Autoradiographic distribution of D3-type dopamine receptors in human brain using [^{3}H]7-hydroxy-N,N-di-n-propyl-2-aminotetralin,'' Brain Res. **648**, 222–228 (1994).

[9] P. Barili, E. Bronzetti, A. Ricci, D. Zaccheo, and F. Amenta, ''Microanatomical localization of dopamine receptor protein immunoreactivity in the rat cerebellar cortex,'' Brain Res. **854**, 130–138 (2000).

[10] W. D. Heiss, G. Pawlik, K. Herholz, R. Wagner, H. Goldner, and K. Wienhard, ''Regional kinetic constants and cerebral metabolic rate for glucose in normal human volunteers determined by dynamic positron emission tomography of [^{18}F]-2-fluoro-2-deoxy-D-glucose,'' J. Cereb. Blood Flow Metab. **4**, 212–223 (1984).

[11] J. Ashburner, J. Haslam, C. Taylor, V. J. Cunningham, and T. Jones ''A cluster analysis approach for the characterization of dynamic PET data,'' in *Quantification of Brain Function Using PET*, edited by R. Myers, V. J. Cunningham, D. Bailey, and T. Jones (Academic, London, 1996), pp. 301–306.

[12] R. N. Gunn, A. A. Lammertsma, and V. J. Cunningham, ''Parametric imaging of ligand-receptor interactions using a reference tissue model and cluster analysis,'' in *Quantitative Functional Brain Imaging with Positron Emission Tomography*, edited by R. E. Carson, M. E. Daube-Witherspoon, and P. Herscovitch (Academic, San Diego, 1998), pp. 401–406.

[13] A. Baune, F. T. Sommer, M. Erb, D. Wildgruber, B. Kardatzki, G. Palm, and W. Grodd, ''Dynamical cluster analysis of cortical fMRI activation,'' Neuroimage **9**, 477–489 (1999).

[14] L.-E. Adam, J. Zaers, H. Ostertag, H. Trojan, M. E. Bellemann, and G. Brix, ''Performance evaluation of the whole-body PET scanner ECAT EXACT HR+ following the IEC standard,'' IEEE Trans. Nucl. Sci. **44**, 1172–1179 (1997).

[15] P. E. Kinahan and J. G. Rogers, ''Analytic 3D image reconstruction using all detected events,'' IEEE Trans. Nucl. Sci. **36**, 964–968 (1989).

[16] R. N. Gunn, A. A. Lammertsma, S. P. Hume, and V. J. Cunningham, ''Parametric imaging of ligand-receptor binding in PET using a simplified reference region model,'' Neuroimage **6**, 279–287 (1997).

[17] M. J. Koepp, R. N. Gunn, A. D. Lawrence, V. J. Cunningham, A. Dagher, T. Jones, D. J. Brooks, C. J. Bench, and P. M. Grasby, ''Evidence for striatal dopamine release during a video game,'' Nature (London) **393**, 266–268 (1998).

[18] T. C. Andrews, R. A. Weeks, N. Turjanski, R. N. Gunn, L. H. A. Watkins, B. Sahakian, J. R. Hodges, A. E. Rosser, N. W. Wood, and D. J. Brooks, ''Huntington's disease progression. PET and clinical observations,'' Brain **122**, 2353–2363 (1999).

[19] R. O. Duda, P. E. Hart, and D. G. Stork, *Pattern Classification*, 4th ed. (Wiley, New York, 2001), Chap. 10.

[20] J. Waldemark, ''An automated procedure for cluster analysis of multivariate satellite data,'' Int. J. Neural Syst. **8**, 3–15 (1997).

[21] A. Wichert, B. Abler, J. Grothe, H. Walter, and F. T. Sommer, ''Exploratory analysis of event-related fMRI demonstrated in a working memory study,'' in *Exploratory Analysis and Data Modeling in Functional Neuroimaging*, edited by F. T. Sommer and A. Wichert (MIT, Boston, MA, 1996), pp. 77–108.

[22] G. Tarantola, F. Zito, and P. Gerundini, ''PET instrumentation and reconstruction algorithms in whole-body applications,'' J. Nucl. Med. **44**, 756–769 (2003).

[23] M. Landmann, S. N. Reske, and G. Glatting, ''Simultaneous iterative reconstruction of emission and attenuation images in positron emission tomography from emission data only,'' Med. Phys. **29**, 1962–1967 (2002).

[24] M. Landmann and G. Glatting, ''Quantitative image reconstruction in PET from emission data only using cluster analysis,'' Z. Med. Phys. **13**, 269–274 (2003).

[25] G. Glatting, C. Werner, S. N. Reske, and M. E. Bellemann, ''ROC analysis for assessment of lesion detection performance in 3D PET: Influence of reconstruction algorithms,'' Med. Phys. **30**, 2315–2319 (2003).

[26] C. Werner, G. Glatting, and M. E. Bellemann, ''Assessment of image reconstruction parameters in PET using physical and statistical figures of merit,'' Biomed. Tech. **47**(Suppl. 1), 463–466 (2002).